

## Charge transfer interaction of organic $\pi$ -acceptors with the anti-hyperuricemic drug allopurinol: Insights from IR, Raman, $^1\text{H}$ NMR and $^{13}\text{C}$ NMR spectroscopies

MOAMEN S. REFAT<sup>1,2\*</sup>  
HOSAM A. SAAD<sup>1,3</sup>  
ABDEL MAJID A. ADAM<sup>1</sup>  
MOHAMED A. AL-OMAR<sup>4</sup>  
AHMED M. NAGLAH<sup>4,5</sup>

<sup>1</sup> Department of Chemistry  
Faculty of Science  
Taif University, Al-Haweiah, P.O. Box 888  
Zip Code 21974, Taif, Saudi Arabia

<sup>2</sup> Department of Chemistry  
Faculty of Science  
Port Said University, Port Said, Egypt

<sup>3</sup> Department of Chemistry  
Faculty of Science  
Zagazig University, Zagazig, Egypt

<sup>4</sup> Department of Pharmaceutical Chemistry  
Drug Exploration & Development Chair  
College of Pharmacy, King Saud University  
Riyadh 11451, Saudi Arabia

<sup>5</sup> Peptide Chemistry Department  
Chemical Industries Research Division  
National Research Centre  
12622-Dokki, Cairo, Egypt

Accepted July 25, 2016

Published online August 2, 2016

The topic of charge-transfer (CT) complexation of vital drugs has attracted considerable attention in recent years owing to their significant physical and chemical properties. In this study, CT complexes derived from the reaction of the anti-hyperuricemic drug allopurinol (Allop) with organic  $\pi$ -acceptors [(picric acid (PA), dichlorodicyanobenzoquinone (DDQ) and chloranil (CHL)] were prepared, isolated and characterized by a range of physicochemical methods, such as IR, Raman,  $^1\text{H}$  NMR and  $^{13}\text{C}$  NMR spectroscopy. The stoichiometry of the complexes was verified by elemental analysis. The results show that all complexes that were formed were based on a 1:1 stoichiometric ratio. This study suggests that the complexation of Allop with either the DDQ or CHL acceptor leads to a direct  $\pi \rightarrow \pi^*$  transition, whereas the molecules of Allop and PA are linked by intermolecular hydrogen-bonding interactions.

**Keywords:** allopurinol,  $\pi$ -acceptor, charge-transfer, proton-transfer

Allopurinol (Allop, 4-hydroxypyrazolo-[3,4-*d*]-pyrimidine, Fig. 1), an anti-hyperuricemic drug, is a structural isomer of hypoxanthine (6-hydroxypurine), which is both a substrate and an inhibitor for xanthine oxidase (1). It is rapidly oxidized *in vivo* to 4,6-dihydroxypyrazolo[3,4-*d*]pyrimidine (oxypurinol), which is a structural isomer of xanthine (2,6-dihydroxypurine) and which is excreted in the urine (1). Allop has been used in mod-

\* Correspondence; e-mail: msrefat@yahoo.com

ern therapy of gout and prevention of the tumor lysis syndrome (2, 3). Allopurinol is currently in the first line urate-lowering treatment, prescribed for patients with guidelines and chronic gout recommendations, starting at a low dose and titrating it upwards until a target urate level is reached (4, 5). Also, Allopurinol acts as a scavenger for toxic hydroxyl free radicals and chelates non-protein-bound (pro-radical) iron (6). It has been found to reduce free-radical formation in both pig and human fetuses (7). Studies have also shown that Allopurinol effectively protects the brain from ischemia and reperfusion-induced injuries caused by oxidative stress in the brain, intestine, kidney and heart (8, 9).

Studies of the charge-transfer (CT) or proton-transfer (PT) interactions of drugs have attracted considerable interest and have become a popular area of research because of their unique physical and chemical properties and wide range of applications (10). The chemistry of these interactions has received considerable attention in pharmacology, chemistry, biology and medicine. They play crucial roles in many processes; therefore, understanding these interactions is important for the understanding of drug-receptor binding and the drug's mechanism of action as well as for obtaining quantitative estimates of drugs (10–12).

During the last decade, considerable efforts were focused on the interactions between drugs or organic donors and acceptors both in the solid state and in solution. For example, Singh and Ahmad (13) studied the interaction between *p*-nitroaniline as a donor and benzoic acid as an acceptor in different polar solvents. Selvakumar *et al.* (14) studied the optical and thermal properties of a 3-nitroanilinium trichloroacetate as a new CT complex, whereas Singh *et al.* (15) prepared a new CT crystal by the interaction between 2,2'-bipyridine as a donor and 3,5-dinitrosalicylic acid as an acceptor. Adam (16) synthesized new nano-structured complexes from the reactions between reserpine and quinidine with chloranilic acid. For several years, our group investigated the synthesis, characterization and application of various CT and PT interactions. For example, the interactions between theophylline (10) and metronidazole (17) with different types of  $\sigma$ - and  $\pi$ -acceptors were studied. In our previous study, we determined the content of Allopurinol in some pharmaceutical preparations spectrophotometrically *via* CT interaction between Allopurinol and 3,6-dichloro-2,5-dihydroxy-*p*-benzoquinone and 2,3-dichloro-5,6-dicyano-*p*-benzoquinone in acetonitrile (18).

As a continuation of this study, and as a part of our continuing interest in this field, in this work, we originally report the structural chemistry of CT complexes formed by intermolecular interactions of Allopurinol with the organic  $\pi$ -acceptors [*i.e.*, picric acid (PA), 2,3-dichloro-5,6-dicyano-1,4-benzoquinone (DDQ) and chloranil (CHL)] in 1:1 methanol-chloroform as a binary solvent system, in order to provide basic data that can be used to determine Allopurinol in pharmaceutical preparations using different acceptors and different solvents.

## EXPERIMENTAL

### *Reagents and equipments*

All the chemicals used were of analytical grade and were used as purchased without further purification. Allopurinol (purity > 99 %) and the organic acceptors, picric acid (purity  $\geq$  98 %), 2,3-dichloro-5,6-dicyano-1,4-benzoquinone (purity > 98 %) or chloranil (purity  $\geq$  99 %) (Fig. 1) were purchased from Sigma-Aldrich Chemical Co. (USA).

C, H and N were analyzed using a Perkin-Elmer 2400 series CHN micro analyzer (USA) in order to obtain the stoichiometry of the interaction. The IR spectra of the products

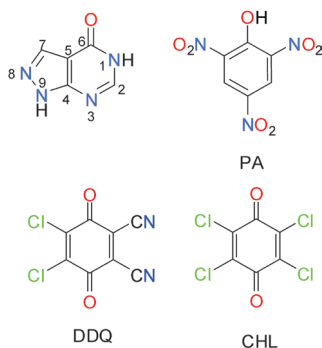


Fig. 1. Chemical structures of drug allopurinol (Allop) and the organic  $\pi$ -acceptors: picric acid (PA), 2,3-dichloro-5,6-dicyano-1,4-benzoquinone (DDQ) and chloranil (CHL).

(KBr discs) were measured at room temperature using a Shimadzu FT-IR spectrophotometer (Japan) over the range of  $4000\text{--}400\text{ cm}^{-1}$  with 30 scans at  $2\text{ cm}^{-1}$  resolution. The Raman laser spectra of the products were acquired on a Bruker FT-Raman spectrophotometer equipped with a 50-mW laser (Bruker, Germany).  $^1\text{H}$  and  $^{13}\text{C}$  NMR spectra were collected on a Bruker DRX-250 spectrometer operating at 600 MHz (Bruker). Measurements were performed at ambient temperature using dimethylsulfoxide ( $\text{DMSO-}d_6$ ) as the solvent and tetramethylsilane (TMS) as the internal reference.

### Syntheses

A typical procedure for the preparation of CT complexes is briefly described as follows. First, 2 mmol of Allop donor (in three beakers) and 2 mmol of each acceptor (PA, DDQ or CHL) were dissolved separately in 20 mL of a 1:1 methanol-chloroform mixture. The solutions were heated until completely dissolved. The Allop donor and the PA, DDQ and CHL acceptors were completely dissolved in 20 mL of a solvent mixture (methanol-

Table I. Elemental analyses of the synthesized CT complexes

Compound	Molecular formula	$M_r$	Elemental analysis (%)						Color
			C		H		N		
			Found	Calc.	Found	Calc.	Found	Calc.	
Allop free	$\text{C}_5\text{H}_4\text{N}_4\text{O}$	136.11	44.00	44.08	2.91	2.94	41.25	41.14	White
Allop-PA complex	$\text{C}_{11}\text{H}_7\text{N}_7\text{O}_8$	365.21	35.97	36.14	1.88	1.92	26.90	26.83	Light yellow
Allop-DDQ complex	$\text{C}_{13}\text{H}_4\text{Cl}_2\text{N}_6\text{O}_3$	363.11	43.05	42.96	1.17	1.10	22.98	23.13	Reddish-brown
Allop-CHL complex	$\text{C}_{11}\text{H}_4\text{Cl}_4\text{N}_4\text{O}_3$	381.99	34.61	34.55	1.00	1.05	14.73	14.66	Yellowish-brown

chloroform, 1:1) at 60 °C. Then the solution of the Allop donor was added to the solution of each acceptor. The resulting mixtures were stirred at room temperature for approximately 0.5 h. Allop-PA, Allop-DDQ, and Allop-CHL products precipitated as light yellow, red-dish-brown and yellowish-brown solid, respectively. The formed products were isolated, filtered, and further purified using the solvent mixture to obtain pure products. The products were then collected and dried *in vacuo* for 48 h.

## RESULTS AND DISCUSSION

### *Stoichiometry of the interaction*

Elemental analyses, molar ratio and color of the synthesized CT complexes are shown in Table I. The stoichiometry of the interaction between the drug Allop and the acceptors (PA, DDQ or CHL) was found to be 1:1, so the structures of the CT complexes were formulated to be [(Allop<sup>+</sup>)(PA<sup>-</sup>)], [(Allop)(DDQ)] and [(Allop)(CHL)].

### *Spectral characterization*

Structures of the synthesized CT complexes have been confirmed by IR,  $^1\text{H}$  and  $^{13}\text{C}$  NMR spectral data. The data obtained by these techniques are consistent with each other and support the suggested structures.

*Vibrational spectroscopy.* – Table II shows characteristic IR spectral bands of free Allop and its CT complexes. The IR spectrum of free Allop was characterized by principal ab-

Table II. Characteristic IR spectral bands ( $\text{cm}^{-1}$ ) of Allop free and its CT complexes

Allop free	CT complex			Assignment
	Allop-PA	Allop-DDQ	Allop-CHL	
–	3448m	–	–	$\nu(\text{N-H} \cdots \text{O})$
3167ms	3166m	3161w	3166w	$\nu(\text{N-H})$ ; of Allop
–	2693m	–	–	$\nu(\text{N-H} \cdots \text{O})$
–	–	2228m	–	$\nu(\text{C}\equiv\text{N})$
1765m	1765w	1744w	1736w	$\nu_{\text{as}}(\text{C=O})$
1699s	1700vs	1704vs	1689vs	$\nu_{\text{s}}(\text{C=O})$
1593s	1592vs	1596vs	1590s	$\delta_{\text{def}}(\text{N-H})$ ; of Allop
1479s	1431ms	1477ms	1479ms	$\nu(\text{C=N})$ ; of Allop
1388ms	1366m	1362m	1364m	$\nu(\text{C=C})$
1235s	1236s	1227s	1232ms	$\nu_{\text{as}}(\text{C-N})$

s – strong, w – weak, m – medium, v – very,

n – stretching,  $n_{\text{s}}$  – symmetrical stretching,  $n_{\text{as}}$  – asymmetrical stretching, d – bending.

sorption peaks at  $3167\text{ cm}^{-1}$  for  $\nu(\text{N-H})$ ,  $2992$ ,  $2943$  and  $2871\text{ cm}^{-1}$  for C–H symmetric and asymmetric stretching,  $1765$  and  $1699\text{ cm}^{-1}$  for  $\nu(\text{C=O})$ ,  $1593\text{ cm}^{-1}$  for  $d_{\text{def}}(\text{N-H})$ ,  $1479\text{ cm}^{-1}$  for  $\nu(\text{C=N})$ ,  $1388\text{ cm}^{-1}$  for  $\nu(\text{C=C})$  and  $1235\text{ cm}^{-1}$  for  $\nu(\text{C-N})$ . The IR spectrum of the Allop-PA complex is characterized by a medium band at  $2693\text{ cm}^{-1}$ . This band is attributed to  $\nu(\text{N-H})$  and confirms migration of the PA proton towards the nitrogen (C=N) of the Allop pyrazole ring to form an intermolecular H-bonded ion pair ( $^+\text{N-H}\cdots\text{O}^-$ ). In general, intermolecular H-bonding in the proton-transfer complex is expected at around  $3400\text{ cm}^{-1}$  (19). The bands observed at around  $3448\text{ cm}^{-1}$  are due to the stretching vibration of  $^+\text{N-H}\cdots\text{O}^-$  and are the evidence of hydrogen bonding in these complexes. In addition, the characteristic band of  $\nu(\text{C=N})$  vibration observed at  $1479\text{ cm}^{-1}$  in the spectrum of free Allop shifts to  $\sim 1431\text{ cm}^{-1}$  in Allop-PA. The observed shift of the  $\nu(\text{C=N})$  band upon complexation suggests that this group participated directly in complexation. All these observations indicate the presence of hydrogen bonding in this complex (13–16). When DDQ and CHL acceptor complexed with Allop, the vibrational frequencies  $\nu(\text{N-H})$ ,  $d_{\text{def}}(\text{N-H})$  and  $\nu(\text{C=N})$  of Allop slightly shift, which indicates that these groups do not participate in the complexation. The cyano, carbonyl and chloro groups in the DDQ or CHL acceptors are electron withdrawing, removing electron density from the aromatic ring and thereby causing it to become an electron-accepting moiety. Instead, Allop contains high electron density over the pyrazole ring (20–22). Fig. 2 shows the representative laser Raman spectra of free Allop and the Allop-PA complex. The Raman spectrum of the free Allop was characterized by principal absorption peaks at  $3101\text{ cm}^{-1}$  for  $\nu(\text{N-H})$ ,  $1696$  and  $1609\text{ cm}^{-1}$  for  $\nu(\text{C=O})$ ,  $1577\text{ cm}^{-1}$  for  $d_{\text{def}}(\text{N-H})$ ,  $1484$

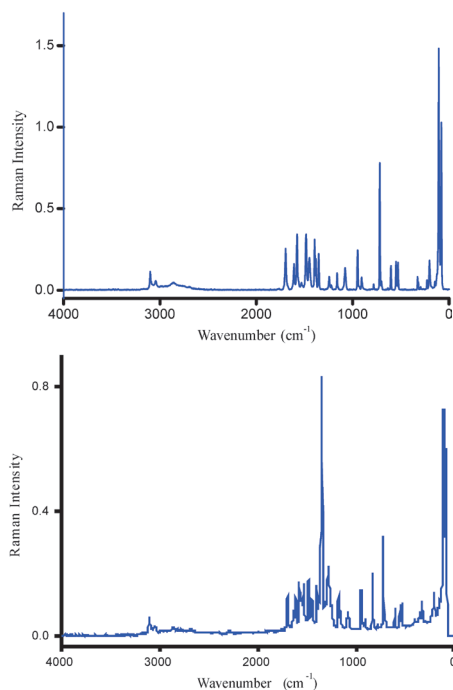


Fig. 2. Laser Raman spectra of: a) free Allop and b) its complex with picric acid.

$\text{cm}^{-1}$  for  $\nu(\text{C}=\text{N})$ ,  $1395\text{ cm}^{-1}$  for  $\nu(\text{C}=\text{C})$  and  $1244\text{ cm}^{-1}$  for  $\nu(\text{C}-\text{N})$ . The strong sharp band observed at  $718\text{ cm}^{-1}$  is assigned to  $d(\text{C}-\text{N})$  out-of-plane bending. The Raman spectrum for the PA complex showed a strong band at  $1346\text{ cm}^{-1}$ , which clearly corresponds to the  $\text{C}=\text{C}$  ring stretching mode. The vibrational modes of  $\nu(\text{C}-\text{N})$  for this complex appear at  $1279\text{ cm}^{-1}$  and the intense sharp band observed at  $718\text{ cm}^{-1}$  corresponds to the out-of-plane bending  $d(\text{C}-\text{N})$ .

*$^1\text{H}$  and  $^{13}\text{C}$  NMR spectroscopy.* – Tables III and IV show the  $^1\text{H}$  and  $^{13}\text{C}$  NMR chemical shifts ( $d$ , ppm) for Allop free and its CT complexes, respectively. Figs. 3 and 4 show the  $^1\text{H}$  and  $^{13}\text{C}$  NMR spectra of Allop-PA and Allop-DDQ complex, respectively. According to the  $^1\text{H}$  NMR spectrum of free Allop, the proton of the pyrimidine ring N-H was observed as a singlet signal at 3.84 ppm, and that of pyrazole ring N-H appeared as a singlet at 12.87 ppm (18). The signal due to the phenolic proton ( $-\text{OH}$ ) of the PA acceptor, which is observed at  $d \sim 11.94$  ppm (10) in the spectrum of the free PA acceptor, is no longer observed. Instead, a new signal is located at approximately  $\sim 6.83$  ppm. This singlet signal is assigned to the  $^*\text{N-H}$  proton formed by proton transfer from the  $-\text{OH}$  group of PA to the nitrogen atom of the Allop pyrazole ring. The singlet peaks observed at  $\sim 8.6$  and  $\sim 12.1$  ppm in the DDQ and CHL complexes were assigned to the pyrimidine ring N-H proton and pyrazole ring N-H proton, respectively. We noted that the signal of the pyrimidine ring N-H proton showed very large shifts relative to the analogous peak in the spectrum of free Allop (3.84 ppm). The electronic environments of Allop protons were affected by the existence of the CT interaction between the Allop and DDQ or CHL acceptor molecules. The  $^{13}\text{C}$  NMR

Table III.  $^1\text{H}$  NMR chemical shifts ( $d$ , ppm) for Allop free and its CT complexes

Compound	Assignment					
	1H, Allop: $\text{N}_{(9)}\text{H}$	1H, Allop: $\text{C}_{(2)}\text{H}$	1H, Allop: $\text{C}_{(7)}\text{H}$	1H, Allop: $\text{N}_{(1)}\text{H}$	2H, PA: $\text{C}_{(3,5)}\text{H}$	1H, hydrogen bonding: $^*\text{NH}$
Allop free	3.84	7.97	8.13	12.87	–	–
Allop-PA	8.55	8.09	8.18	12.13	8.60	6.83
Allop-DDQ	8.60	8.09	8.18	12.18	–	–
Allop-CHL	8.58	8.11	8.20	12.10	–	–

Table IV.  $^{13}\text{C}$  NMR chemical shifts ( $d$ , ppm) for Allop free and its CT complexes

Compound	Assignment		
	$\text{C}=\text{O}$	$\text{C}=\text{N}$	$\text{C}=\text{C}$
Allop free	158.1	134.8, 147.8	105.8, 155.0
Allop-PA	160.5	124.4, 141.7	105.5, 125.0, 133.4, 147.8, 153.7, 157.6
Allop-DDQ	155.3	126.7, 141.8	115.3, 120.5, 127.4, 128.2, 128.5, 142.4
Allop-CHL	156.2	124.5, 147.4	119.2, 127.7, 131.5, 132.8

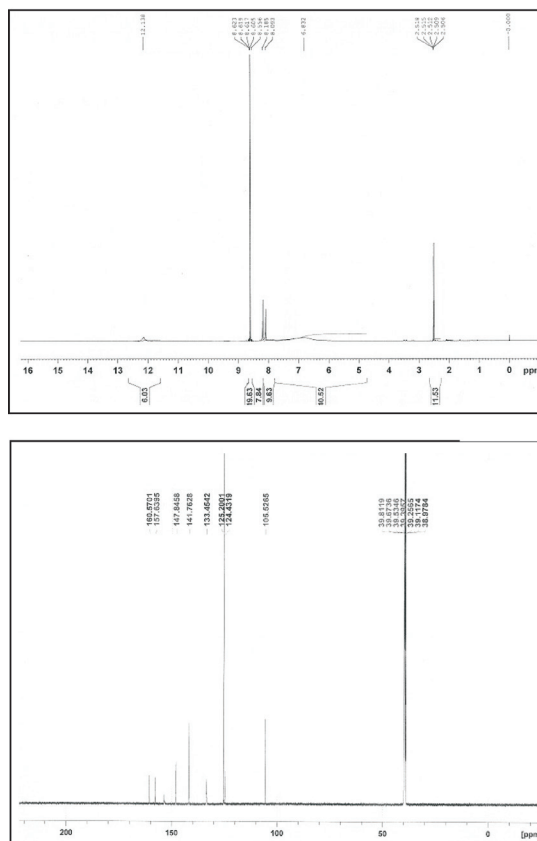


Fig. 3. Spectra of the Allop-PA complex: a)  $^1\text{H}$  and b)  $^{13}\text{C}$  spectrum.

spectrum of free Allop showed five resolved carbon signals. The appearance of nine resonant carbon signals in the  $^{13}\text{C}$  NMR spectra of the Allop-PA and Allop-DDQ complexes, and seven for the Allop-CHL complex is consistent with the proposed molecular structure of these complexes. For all complexes, common changes in the values of  $^{13}\text{C}$  chemical shifts in Allop can be observed as a result of its complexation with organic acceptors.

### Complexation pathway

In a previous study, we found that Allop forms a yellow solid complex with DDQ in acetonitrile *via* 1:1 interaction, and the CT interaction occurs through  $n\text{-}\pi^*$  transition with deprotonation of NH group of Allop, to only one of the CN groups of DDQ, by forming intermolecular hydrogen bonding (18). In this study, however, Allop forms a reddish-brown solid complex with DDQ in methanol-chloroform mixture, but the IR data indicate that the interaction occurs through  $\pi\text{-}\pi^*$  transition *via* the pyrazole ring of Allop and the aromatic ring of DDQ. This difference in complexation pathway could be attributed to the

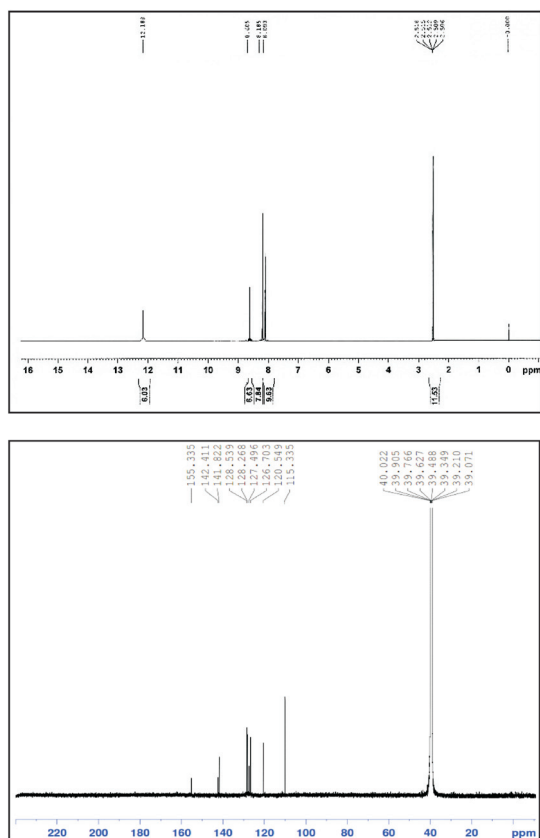


Fig. 4. Spectra of the Allop-DDQ complex: a)  $^1\text{H}$  and b)  $^{13}\text{C}$  spectrum.

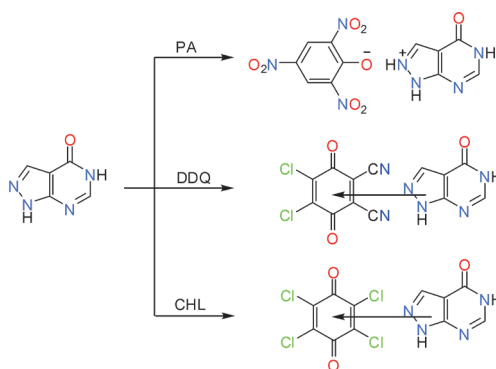


Fig. 5. Proposed structural formula of the proton-transfer complex Allop-PA and charge-transfer complexes Allop-DDQ and Allop-CHL (for the acronyms see above).



solvent effect. Complexation of Allop with CHL acceptor also leads to a direct  $\pi \rightarrow \pi^*$  transition via the pyrazole ring of the Allop and the aromatic ring of CHL, whereas hydrogen bonding with proton transfer is observed between Allop and PA acceptor. Fig. 5 illustrates the proposed structures of Allop complexes with PA, DDQ and CHL acceptors.

## CONCLUSIONS

Structures of the synthesized CT complexes have been confirmed by IR,  $^1\text{H}$  and  $^{13}\text{C}$  NMR spectral data. The data obtained by these techniques are consistent with each other and support the suggested structures. Our findings indicated that the molecules in the Allop-DDQ and Allop-CHL complexes are linked by charge-transfer interactions, whereas the rings of Allop with PA are linked by intermolecular hydrogen-bonding interaction. In further investigations, we will shed some new light on the biological activities of the Allop CT complexes.

*Acknowledgments.* – The project was financially supported by King Saud University, Vice Deanship of Research Chairs.

## REFERENCES

1. A. Chalmers, R. Parker, H. A. Simmonds, W. Snedden and W. E. Watts, The conversion of 4-hydroxypyrazolo[3,4-d]pyrimidine (allopurinol) into 4,6-dihydroxypyrazolo[3,4-d]pyrimidine (oxipurinol) *in vivo* in the absence of xanthine-oxygen oxidoreductase, *Biochem. J.* **112** (1969) 527–532.
2. M. Tabandeh, S. Ghassamipour, H. Aqababa, M. Tabatabaei and M. Hasheminejad, Computational design and synthesis of molecular imprinted polymers for selective extraction of allopurinol from human plasma, *J. Chromatogr. B* **898** (2012) 24–31; DOI: 10.1016/j.jchromb.2012.04.009.
3. T. F. Yu and A. B. Gutman, Effect of allopurinol (4-hydroxypyrazolo-(3,4-d)pyrimidine) on serum and urinary uric acid in primary and secondary gout, *Am. J. Med.* **37** (1964) 885–891; DOI: 10.1016/0002-9343(64)90131-7.
4. C. G. Jennings, I. S. Mackenzie, R. Flynn, I. Ford, G. Nuki, R. De Caterina, P. L. Riches, S. H. Ralston and T. M. MacDonald, Up-titration of allopurinol in patients with gout, *Semin. Arthritis Rheum.* **44** (2014) 25–30; DOI: 10.1016/j.semarthrit.2014.01.004.
5. T. R. Mikuls, J. T. Farrar, W. B. Bilker, S. Fernandes, H. R. Schumacher and K. G. Saag, Gout epidemiology: results from the UK general practice research database, 1990–1999, *Ann. Rheum. Dis.* **64** (2005) 267–272; DOI: 10.1136/ard.2004.024091.
6. J. Prickaerts, E. T. Gieling, A. K. Bruder, F. J. van der Staay and T. Vanmierlo, Long-term effects of prenatal allopurinol treatment on brain plasticity markers in low and normal birth weight piglets, *Int. J. Dev. Neurosci.* **33** (2014) 29–32; DOI: 10.1016/j.ijdevneu.2013.11.001.
7. D. N. I. Boda, P. Kiss and H. Orvos, Treatment of mothers with allopurinol to produce therapeutic blood levels in newborns, *Prenatal Neonatal Med.* **4** (1999) 130–134.
8. G. Dong, M. Ren, X. Wang, H. Jiang, X. Yin, S. Wang, X. Wang and H. Feng, Allopurinol reduces severity of delayed neurologic sequelae in experimental carbon monoxide toxicity in rats, *Neurotoxicology* **48** (2015) 171–179; DOI: 10.1016/j.neuro.2015.03.015.
9. A. Torreggiani, M. Tamba, A. Trincherio and G. Fini, A spectroscopic and pulse radiolysis study of allopurinol and its copper complex, *J. Mol. Struct.* **651–653** (2003) 91–99; DOI: 10.1016/S0022-2860(02)00631-2.

10. A. M. A. Adam and M. S. Refat, Nanostructured products of the drug theophylline caused by charge transfer interactions and a binary solvent system: Morphology and nanometry, *J. Mol. Liq.* **209** (2015) 33–41; DOI: 10.1016/j.molliq.2015.05.021.
11. B. K. Bozođlan, S. Tunç and O. Duman, Investigation of neohesperidin dihydrochalcone binding to human serum albumin by spectroscopic methods, *J. Lumin.* **155** (2014) 198–204; DOI: 10.1016/j.jlumin.2014.06.032.
12. M. Saravanabhavan, K. Sathya, V. G. Puranik and M. Sekar, Synthesis, spectroscopic characterization and structural investigations of new adduct compound of carbazole with picric acid: DNA binding and antimicrobial studies, *Spectrochim. Acta A* **118** (2014) 399–406; DOI: 10.1016/j.saa.2013.08.115.
13. N. Singh and A. Ahmad, Synthesis and spectrophotometric studies of charge transfer complexes of p-nitroaniline with benzoic acid in different polar solvents, *J. Mol. Struct.* **1074** (2014) 408–415; DOI: 10.1016/j.molstruc.2014.05.076.
14. E. Selvakumar, A. Chandramohan, G. A. Babu and P. Ramasamy, Synthesis, growth, structural, optical and thermal properties of a new organic salt crystal: 3-nitroanilinium trichloroacetate, *J. Cryst. Growth* **401** (2014) 323–326; DOI: 10.1016/j.jcrysgro.2013.10.053.
15. N. Singh, I. M. Khan, A. Ahmad and S. Javed, Synthesis, crystallographic and spectrophotometric studies of charge transfer complex formed between 2,2'-bipyridine and 3,5-dinitrosalicylic acid, *J. Mol. Liq.* **191** (2014) 142–150; DOI: 10.1016/j.molliq.2013.12.002.
16. A. M. A. Adam, Nano-structured complexes of reserpine and quinidine drugs with chloranilic acid based on intermolecular H-bond: Spectral and surface morphology studies, *Spectrochim. Acta A* **127** (2014) 107–114; DOI: 10.1016/j.saa.2014.02.077.
17. M. S. Refat, H. A. Saad and A. M. A. Adam, Spectral, thermal and kinetic studies of charge-transfer complexes formed between the highly effective antibiotic drug metronidazole and two types of acceptors:  $\sigma$ - and  $\pi$ -acceptors, *Spectrochim. Acta A* **141** (2015) 202–210; DOI: 10.1016/j.saa.2015.01.029.
18. M. S. Refat, G. G. Mohamed and A. Fathi, Spectrophotometric determination of allopurinol drug in tablets: Spectroscopic characterization of the solid CT complexes, *Bull. Korean Chem. Soc.* **31** (2010) 1535–1542; DOI: 10.5012/bkcs.2010.31.6.1535.
19. M. Manikandan, T. Mahalingam, Y. Hayakawa and G. Ravi, Synthesis, structural, spectroscopic and optical studies of charge transfer complex salts, *Spectrochim. Acta A* **101** (2013) 178–183; DOI: 10.1016/j.saa.2012.08.086.
20. I. A. Darwish, J. M. Alshehri, N. Z. Alzoman, N. Y. Khalil and H. M. Abdel-Rahman, Charge-transfer reaction of 1,4-benzoquinone with crizotinib: Spectrophotometric study, computational molecular modeling and use in development of microwell assay for crizotinib, *Spectrochim. Acta A* **131** (2014) 347–354; DOI: 10.1016/j.saa.2014.04.099.
21. H. M. Elqudaby, G. G. Mohamed and G. M. G. El-Din, Analytical studies on the charge transfer complexes of loperamide hydrochloride and trimebutine drugs. Spectroscopic and thermal characterization of CT complexes, *Spectrochim. Acta A* **129** (2014) 84–95; DOI: 10.1016/j.saa.2014.02.110.
22. M. S. Refat, L. A. Ismail and A. M. A. Adam, Shedding light on the photostability of two intermolecular charge-transfer complexes between highly fluorescent bis-1,8-naphthalimide dyes and some  $\pi$ -acceptors: A spectroscopic study in solution and solid states, *Spectrochim. Acta A* **134** (2015) 288–301; DOI: 10.1016/j.saa.2014.06.107.